8 Study of Coulomb-bound πK-pairs

C. Amsler, A. Benelli[4], C. Regenfus, and J. Rochet

in collaboration with:
CERN, Czech Technical University, Institute of Physics and Nuclear Physics Institute ASCR (Czech Republic), Laboratori Nazionali di Frascati, Messina University, Trieste University, KEK, Kyoto Sangyo University, Tokyo Metropolitan University, IFIN-HH (Bucharest), JINR (Dubna), Skobeltsin Institute for Nuclear Physics (Moscow), IHEP (Protvino), Santiago de Compostela University, Bern University.

(DIRAC Collaboration)

The DIRAC experiment at CERN (PS212) is measuring the lifetime of electromagnetically bound $\pi^+\pi^-$- or $\pi^\mp K^\pm$-pairs ($\pi\pi$-atoms or pionium, and πK-atoms). Results for $\pi\pi$-atoms have been published earlier by the DIRAC-I collaboration [1]. The final result for the mean life [2] is 3.15 $\pm$ 0.20 (stat) $\pm$ 0.19 (syst) fs which leads to the determination of the difference in the isospin 0 and 2 $\pi\pi$-scattering lengths with a precision of 4%, namely $|a_0 - a_2| = 0.2533 \pm 0.0079$ (stat) ± 0.0075 (syst) m_π^{-1}, in agreement with results obtained from K-decay into 3π [3] and K-decay into $2\pi e\nu$ [4].

We are mainly involved in the study of πK-atoms (DIRAC-II experiment) for which we developed and built the aerogel Čerenkov counters to distinguish pions from kaons. The mean life of the πK-atom is related to the isospin 1/2 and 3/2 πK scattering lengths ($a_{1/2}$ and $a_{3/2}$) or, more precisely, to the absolute value of the difference between the two scattering lengths, a quantity that was calculated within 5% from Roy-Steiner dispersion-relations [5]. A measurement of the mean life will test low-energy QCD concepts involving the u- and d-quarks for $\pi\pi$, and extending to the s-quark sector for πK. The expected mean life of πK-atoms is 3.7 fs with large uncertainty [6].

Details on the apparatus can be found in Ref. [7] and in previous annual reports. We use the 24 GeV/c proton beam from the PS which traverses a thin Pt- (or Ni-) target. The secondary particles emerging from the target in the forward direction are analyzed in a double-arm magnetic spectro-meter. Electrons and positrons are vetoed by N_2-Čerenkov detectors and muons by scintillation counters behind thick absorbers. Kaons are separated from pions and protons by heavy gas (C_4F_{10}) Čerenkov counters (which fire on pions) and by an aerogel Čerenkov counters (which fires on both pions and kaons, but not not on the more numerous protons). Our group has developed and built the 37ℓ aerogel Čerenkov counter [8] and the gas system for the C_4F_{10} counters [9]. The aerogel detector consists of three independent modules. Two of them have refractive index $n = 1.015$ and are used for kaons between 4 and 5.5 GeV/c. At small angles with respect to the primary beam axis the momenta increases up to 8 GeV/c and hence an aerogel counter with lower refractive index ($n = 1.008$) is used to suppress fast protons.

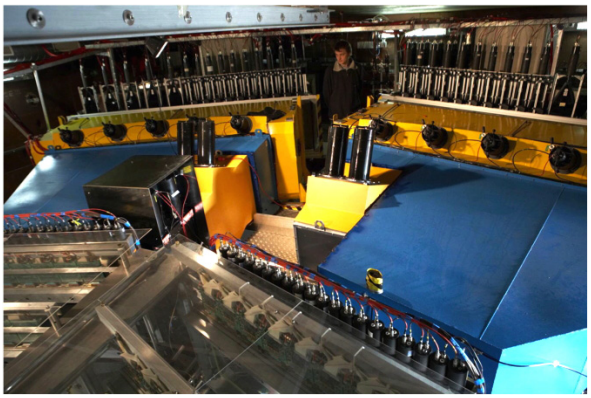

Fig. 8.1 – The DIRAC experiment. The black box on the left houses the aerogel counters. The yellow boxes are the heavy gas counters. The blue boxes contain the N_2 counters. The photomultipliers in the back belong to the detectors rejecting muons.

[4]Visitor from JINR, Dubna

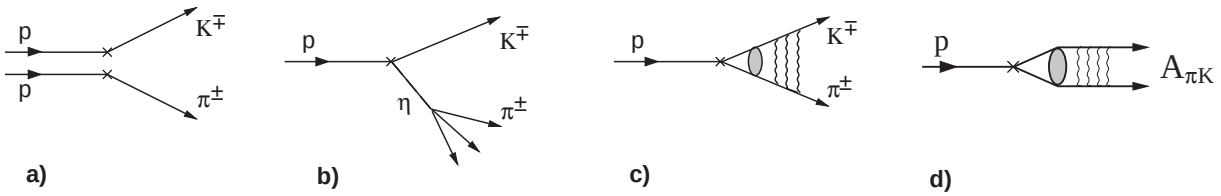

Fig. 8.2 – Production mechanisms of πK-pairs: a) accidental-pairs from two protons; b) non-Coulomb-pairs from long-lived intermediate states such as the η-meson; c) Coulomb-pairs from direct production or from short-lived intermediate states; d) πK-atoms.

A photograph of the equipment downstream of the dipole magnet is shown in Fig. 8.1.

Figure 8.2 shows the four mechanisms which contribute to the production of $\pi^{\pm}K^{\mp}$-pairs. Briefly, πK- (or $\pi\pi$-) atoms produced by incident protons fly in the forward direction and are ionized while crossing the target, leading to a peak from "atomic" pairs at very small relative momenta between the two particles (typically < 3 MeV/c in the c.m.s system). Since ionization competes with other processes such as annihilation, the number of atomic pairs grows with increasing lifetime. Unbound πK-pairs ("Coulomb-pairs") which interact electromagnetically are also produced and their numbers are related to the number of atoms [10]. The background stems from non-Coulomb pairs due to K and π mesons from long-lived resonances (which therefore do not interact), and from accidentals (pairs produced by two different proton interactions).

The DIRAC collaboration observed πK-atoms for the first time with the data collected in 2007 [11]. This result led to a lower limit for the mean life of πK-atoms of 0.8 fs in the $1s$-state, which could be translated into an upper limit of $|a_{1/2} - a_{3/2}| < 0.58\ m_{\pi}^{-1}$. Details can be found in Ref. [11–13].

For the 2007 data we had used only the detectors downstream of the magnet. Three main improvements were implemented for the 2008 – 2010 runs. A scintillation fibre detector (SFD, described below) and microdrift chambers are now available to determine the interaction point in the production target with better precision. The SFD measures tracks with good resolution ($\sigma = 60$ μm), high efficiency (98%) and improves the resolution on the transverse momentum Q_T from 3 MeV/c to 1 MeV/c, which reduces the background by typically a factor of four. ADC's for the aerogel detectors were also not available in the 2007 runs while this information is now recorded and, accordingly, the detection efficiency for kaons with the aerogel and the contamination from protons can be calculated reliably. The detection efficiency for kaons is typically 95% above 5 GeV/c and the contamination from protons around 5%, except for high energy protons close to the beam axis for which the proton contamination rises significantly. However, simulation shows that even a contamination of 100% is not problematic since no enhancement is observed for protons at small relative longitudinal momenta.

Finally, in 2007 the main goal was the observation of πK-atoms and hence a platinum target was chosen for which the production cross section was high. However, for platinum the breakup probability as a function of mean life (53% for 3.7 fs) is flattening off above ~ 4 fs and hence we could only give a lower limit for the mean life. We now use a nickel target for which the dependence between breakup probability and mean life is described by a steeper function, although atoms are produced with a lower cross section.

During 2010 we tuned the Monte Carlo simulation of the scintillation fibre detector (SFD). A sketch of the detector is shown in Fig. 8.3. The detector consists of 3 planes (x, y, and w) of scintillating fibres (diameter 205 μm). The x- and y-planes are made of 8 layers each with 480 fibres while the w-planes contain 3

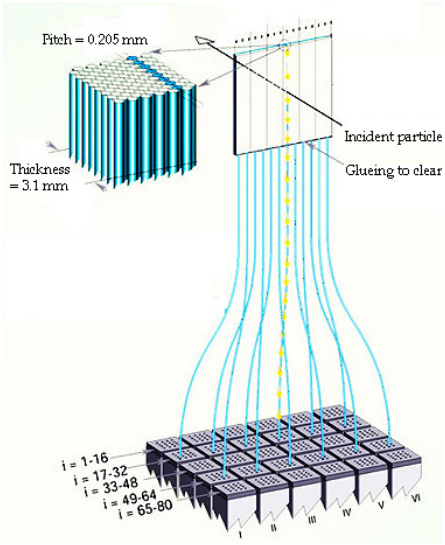

Fig. 8.3 – Layout of the scintillating fibre detector.

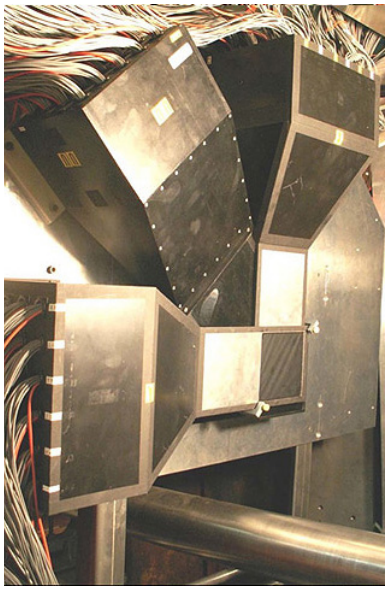

Fig. 8.4 – The scintillating fibre detector.

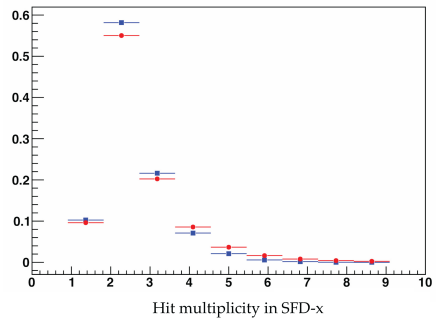

Fig. 8.5 – Hit multiplicity in the SFD x plane.

layers of 320 fibres. The fibres are read out in columns of 8, respectively 3 fibres by 30 × 16 Hamamatsu H6568 photomultipliers. The area covered by each plane is about 10 × 10 cm^2 and contributes only 1% radiation length. The timing resolution is 460 ps. A photograph of the detector is shown in Fig. 8.4.

We now illustrate the performance of the SFD using $\pi^+\pi^-$ data which are more abundant than πK data. The x-plane of the SFD detector was equipped with new readout electronics featuring both TDC's and ADC's. An important software tool was developed using the ADC information, the peak sensing algorithm, which compares the signal amplitudes for neighbouring hits to reduce background. Figure 8.5 compares the measured hit multiplicity with simulation after having applied the peak sensing algorithm. Figure 8.6 shows the distribution of the distance between two tracks measured by the SFD x-plane. In both plots good agreement between data and simulation is observed.

In 2010 we also proceeded with the analysis of the 2008 –2009 data with the upstream detectors, selecting πK events as cleanly as possible. The SFD detector and the nearby ionization hodoscope are used to resolve double tracks. Drift chamber (DC) tracking is performed and only upstream tracks that have hits in the SFD are kept. The distance between the DC extrapolation at the SFD plane and the actual SFD hit has to be smaller than 1 cm. Particle identification using the heavy gas Cerenkov and aereogel detectors is then performed and a precise timing between the two tracks is required. The relative transverse momentum is required to be smaller than $Q_T = 4$ MeV/c, the relative longitudinal momentum less than $|Q_L| = 20$ MeV/c. Figure 8.7 shows the experimental π^+K^- and π^-K^+ distributions with fit results superimposed. The fit includes atomic pairs (red), Coulomb pairs (blue) and non-Coulomb pairs (magenta). The sum of Coulomb and non-Coulomb pairs is shown in black.

A method to measure the energy difference ΔE_ninside between the pionium np- and ns-states was proposed as follows [14]. When moving inside

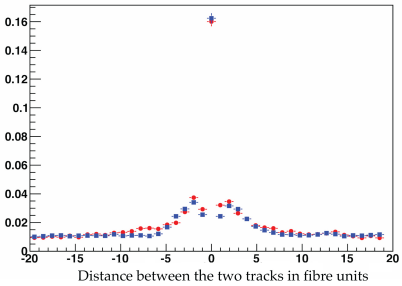

Fig. 8.6 – Distribution of the distance between the π^+ and π^- tracks in the x-plane of the SFD. The measured data are shown in red, the simulation in blue.

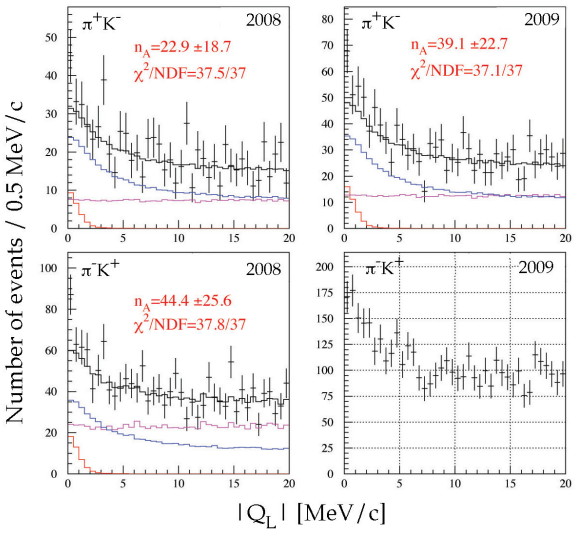

Fig. 8.7 – Distributions of longitudinal relative momentum Q_L for the 2008 and 2009 data. Top: π^+K^-; bottom: π^-K^+. The measured data are shown by the histograms with error bars; the other histograms are described in the text. The analysis of the π^-K^+ data from 2009 is in progress.

the target, the atoms interact with an applied electric field. Some of them leave the target in the $2p$-state. The decay into $\pi^0\pi^0$ being forbidden from p-states the main decay process is $2p - 1s$ radiative transition with subsequent annihilation from $1s$ into $\pi^0\pi^0$. Thus, the mean life of the atom in the $2p$-state is determined by radiative transition, $\tau(2p) \simeq 12$ ps [10], which is much slower than annihilation from ns-states. One can then measure the energy difference ΔE_n by observing the field dependence of the decay rate in the applied electric field. This determines the combination $2a_0 + a_2$ of the $\pi\pi$-scattering lengths. Combining with our measurement from the $1s$-state we will be able to derive a_0 and a_2 separately. This method can also be applied to the πK-system to obtain $a_{1/2}$ and $a_{3/2}$ separately.

During summer 2010 DIRAC took data with excellent detector performance and stable beam from the PS accelerator. DIRAC has been approved to run at least until the end of 2011. More data on πK-atoms will be collected in 2011 together with measurements of the energy difference between the ns and np states of pionium.

[1] B. Adeva *et al.* (DIRAC Collaboration), Phys. Lett. **B 619** (2005) 50.

[2] B. Adeva *et al.* (DIRAC Collaboration), submitted to Phys. Rev. Lett.

[3] J. R. Bately *et al.*, Eur. Phys. J. **C 64** (2009) 589.

[4] J. R. Bately *et al.*, Eur. Phys. J. **C 70** (2010) 635.

[5] P. Büttiker, S. Descotes-Genon, B. Moussallam, Eur. Phys. J. **C 33** (2004) 409.

[6] J. Schweizer, Phys. Lett. **B 587** (2004) 33.

[7] B. Adeva *et al.* (DIRAC Collaboration), Nucl. Instrum. Methods in Phys. Res. **A 515** (2003) 467.

[8] Y. Allkofer *et al.*, Nucl. Instr. Meth. in Phys. Res. **A 582** (2007) 497; Y. Allkofer *et al.*, Nucl. Instr. Meth. in Phys. Res. **A 595** (2008) 84.

[9] S. Horikawa *et al.*, Nucl. Instr. Meth. in Phys. Res. **A 595** (2008) 212.

[10] L. L. Nemenov, Sov. J. Nucl. Phys. **41** (1985) 629; L. Afanasyev and O. Voskresenskaya, Phys. Lett. **B 453** (1999) 302.

[11] B. Adeva *et al.* (DIRAC Collaboration), Phys. Lett. **B 674** (2009) 11.

[12] Y. Allkofer, PhD Thesis, University of Zurich (2008).

[13] C. Amsler, Proc. of Science PoS EPS-HEP (2009) 078.

[14] Addendum to PS212 (09/02/11): CERN-SPSC-2011-001 (SPSC-P-284 Add. 5).